DOI 10.1007/s10778-015-0695-5
International Applied Mechanics, Vol. 51, No. 3, May, 2015

MEASURING THE AMPLITUDES AND PHASES OF VIBRATIONS OF PIEZOCERAMIC STRUCTURAL ELEMENTS

N. A. Shul'ga and V. L. Karlash

The results on forced electromechanical vibrations of piezoceramic half-disks in some range of frequencies are systemized and generalized. Much attention is drawn to new experimental methods for studying the amplitude-frequency and phase-frequency characteristics

Keywords: piezoceramic half-disk, forced vibrations, admittance, amplitude-frequency and phase-frequency characteristics, phase ratio

Introduction. Problems of the resonant and forced vibrations of piezoelectric bodies have been in the focus of attention of scientists for many decades due to the high efficiency of electromechanical energy conversion [1–5, 7–9, 11–16, 18–30, etc.]. In tests on piezoelectric vibrators, the mass, static capacitance, dimensions, characteristic (resonant and antiresonant) frequencies of and the voltage drop across the piezoelectric element and/or the pull-up resistor are directly measured [7–9, 11–15, 19–23, etc.] to determine, by various methods, the components of admittance and the active (real) and reactive (imaginary) components of the material constants. There are no methods for the direct measurement of the active and reactive components of admittance; therefore, they have to be determined indirectly, i.e., calculated by various approximate formulas.

The recent studies [28–30] show that the behavior of piezoelectric vibrators at high power strongly depends on the type of electric loading. The admittance–frequency response at voltage of constant amplitude is essentially nonlinear, including abrupt drops and jumps. Such nonlinearity is absent if the current is of constant amplitude [30].

The quest for ways to measure the electroelastic and viscoelastic coefficients of piezoelectric vibrators is still ongoing. A method for determining the Q-factor and piezoelectric modulus by differentiating the frequency-dependent active component of the admittance with respect to frequency is described in [5]. An interesting combined experimental/numerical procedure was proposed in [1] where the active components of the electroelastic material constants of piezoceramics are determined by measuring the resonant frequencies of various vibration modes of a rectangular rod from which a square plate is then cut out. In [25, 26], it was shown that the values of the Q-factor at resonance (Q_a) and antiresonance (Q_b) are different, and $Q_a < Q_b$.

Here we further develop experimental methods by searching ways of studying phase–frequency responses in some frequency range, generalizing and comparing resonance/antiresonance methods, and assessing the accuracy of values of some most frequently used parameters. For example, we will show that the classical two-port network (Mason circuit) provides tolerable errors only at characteristic frequencies, whereas in frequency ranges below resonance and between neighboring resonances there are considerable phase shifts between the current and the voltage drop across the piezoelectric element. An advanced Mason circuit with an additional switch allows reducing the effect of phase shifts. Combining the resonance–antiresonance [4, 14, 21] and piezotransformer transducer [8, 13, 18, 19] methods considerably simplifies experiments and improves their accuracy.

1. Response of a Piezoceramic Element to an External Electric Load. There are several methods to measure the resonant frequencies of piezoelectric structural elements. All of them are approximate. Most popular is the passive two-port

S. P. Timoshenko Institute of Mechanics, National Academy of Sciences of Ukraine, 3 Nesterova St., Kyiv, Ukraine 03057, e-mail: karlashv@ukr.net. Translated from Prikladnaya Mekhanika, Vol. 51, No. 3, pp. 122–133, May–June 2015. Original article submitted March 5, 2012.

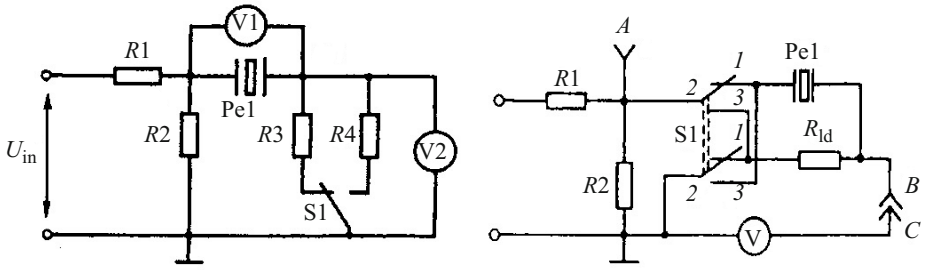

a *b*

Fig. 1

network (so-called Mason circuit) in which the piezoelectric element is connected in series with a pull-up resistor (Fig. 1a). The advantages and disadvantages of this method are detailed in [7, 8, 14, 20].

The admittance–frequency response of a thin piezoceramic half-disk in a frequency range 20–100 kHz were obtained in [21] using a Mason circuit (Fig. 1b) modified so as to switch the grounding point of the measuring circuit. This makes it possible to measure the voltage drop across either the piezoelectric element or the load.

To excite mechanical vibrations of the piezoelectric element, it is necessary to apply to its electrodes some voltage from an external ultrasonic generator. Resulting from the inverse piezoelectric effect, the electric field causes mechanical deformation of the piezoelectric element. The frequency of electromechanical vibrations is equal to that of the exciting field. The voltage U_{pe} applied to the piezoelectric element causes a current I_{pe}. It is well known that a voltage drop can be measured with a voltmeter, while a current with an ampermeter [6, 10, 12]. A voltmeter is always connected in parallel to the electric circuit of interest, while an ampermeter is connected in series. Neither of them must affect the measured result. For this reason, the internal resistance of the voltmeter must be many times higher than the resistance of the circuit of interest not to distort the measured value of the current. The ampermeter, vice versa, must have very low resistance not to distort the measured voltage drop. The current/voltage ratio is, by definition, admittance Y_{pe},

$$Y_{pe} = I_{pe} / U_{pe}. \tag{1}$$

It is impossible to directly measure the voltage drop across and the current through the piezoelectric element because there are no ultrasonic ampermeters and voltmeters. The current through the piezoelectric element is measured indirectly from the voltage drop across a special resistor connected in series. The Mason circuit usually includes two voltmeters [3, 8, 11, 13, 19], one parallel to the piezoelectric element, and the other parallel to the pull-up resistor.

As the generator is tuned, the readings of both voltmeters change, but their vector sum is always equal to the voltage drop U_{R2} across the output resistor $R2$ of the matching divider. For this reason, one of the voltmeters is sometimes connected in parallel to the resistor $R2$, and the voltage drop across the piezoelectric element is equal to the difference between the voltage drop across the resistor $R2$ and the voltage drop across the pull-up resistor. As the frequency increases, the current through the piezoelectric element increases too and so does the voltage drop across the pull-up resistor. Far from the resonance (at low frequency), the current through the piezoelectric element is related to its static recharge and to the increase in the capacitive susceptance with increasing frequency. The static capacitance of the piezoelectric element is due to its basic electrodes, which are often on its main faces. The closer the generator frequency to one of the resonances of the piezoelectric element, the sharper the changes in the readings of the voltmeters. At the frequency f_m of the maximum input admittance Y_m, which is close to the resonant frequency f_r, the voltage drop U_m across the resistor $R3$ reaches a maximum many times higher than the capacitive component. At the frequency f_n of the minimum admittance Y_n, which is close to the antiresonant frequency f_a, the voltage drop U_n across the resistor $R4$ reaches a minimum. The admittance of the piezoelectric element at any frequency results from the combination of the piezoelectric effect and static capacitance. The frequency of the maximum voltage drop across the pull-up resistor differs a little from the resonant frequency because of the effect of the static self-capacitance of the piezoelectric element.

The admittance Y of the piezoelectric element consists of real G (active) and imaginary B (reactive) components. For example, before the first radial resonance, the capacitive susceptance (of the equivalent capacitor C_0) of the piezoelectric element makes the predominant contribution to the admittance of the thin piezoceramic disk with solid electrodes on the main

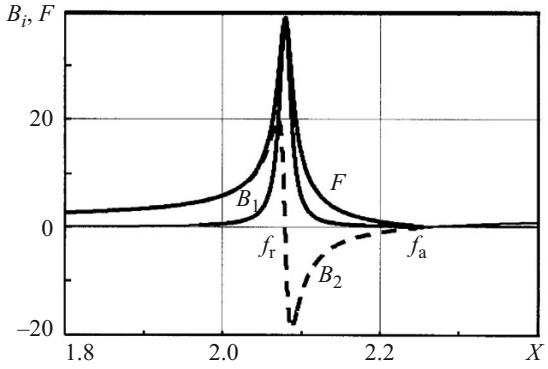

Fig. 2

faces (Fig. 2), and only near the resonance, the active component (conductivity) induced by mechanical stresses is vectorally added to it [14]. At some point, the reactive component is maximum and equal to the active component. Then the active component continues to increase, while the reactive component decreases. At the resonant frequency, the active component becomes maximum, whereas the reactive drops to zero. After that, the reactive component reverses sign, reaches a negative maximum, and decreases to zero. The active component decreases to zero as well. The admittance reaches a minimum at the point where the reactive component becomes zero for the second time and then again the contribution of the capacitive susceptance becomes predominant. The figure also indicates that the points of maxima of the conductance and admittance practically coincide with each other and with the first point at which the susceptance becomes zero. Also, the points of minima of the conductivity and admittance coincide with the second point at which the susceptance again becomes zero. The maximum of the admittance is much sharper than its minimum. For that very reason (for more accurate detection of minima), the pull-up resistors $R3$ and $R4$ in the Mason circuit have different resistances. Usually, the resistance of $R3$ is several Ohms, while the resistance of $R4$ can reach several hundreds of Ohms.

The voltage drop across the piezoelectric element can most easily be determined indirectly as the difference between the voltage drop across the output resistor $R2$ of the matching divider (the input potential difference of the measuring circuit) and the voltage drop across the pull-up resistor:

$$U_{\text{pe}} \cong U_{R2} - U_R . \tag{2}$$

Thus, the admittance of the piezoelectric element at any frequency can be determined from the approximate formula

$$Y_{\text{pe}} = U_R / R(U_{R2} - U_R). \tag{3}$$

This formula ensures adequate accuracy at characteristic (resonant and antiresonant) frequencies, but beyond these frequencies, considerable phase distortions are possible.

If the advanced Mason circuit is used, formula (1) becomes

$$Y_{\text{pe}} = U_R / (U_{\text{pe}} R). \tag{4}$$

The phase differences between the current through and the voltage drop across the piezoelectric element are the same, but they do not affect the accuracy of measurements.

Replacing the pull-up resistor with a capacitor C_{ld} produces good results. In this case, the admittance Y_{pe} of the piezoelectric element at a frequency f is determined in terms of the ratio of the voltage drops across the capacitor (U_{c}) and the piezoelectric element (U_{pe}):

$$Y_{\text{pe}} = 2\pi f C_{\text{ld}} U_{\text{c}} / U_{\text{pe}} U_{\text{pe}} . \tag{5}$$

The capacitance C_{ld} can be added to the measuring section of the Mason circuit or its modifications, as well as the pull-up resistor, through either a load or a transfer element. The voltage drops across the capacitor and the piezoceramic half-disk were measured for several values of C_{ld}: equal to, much lower, and much higher than the static capacitance C_0. If the capacitor is

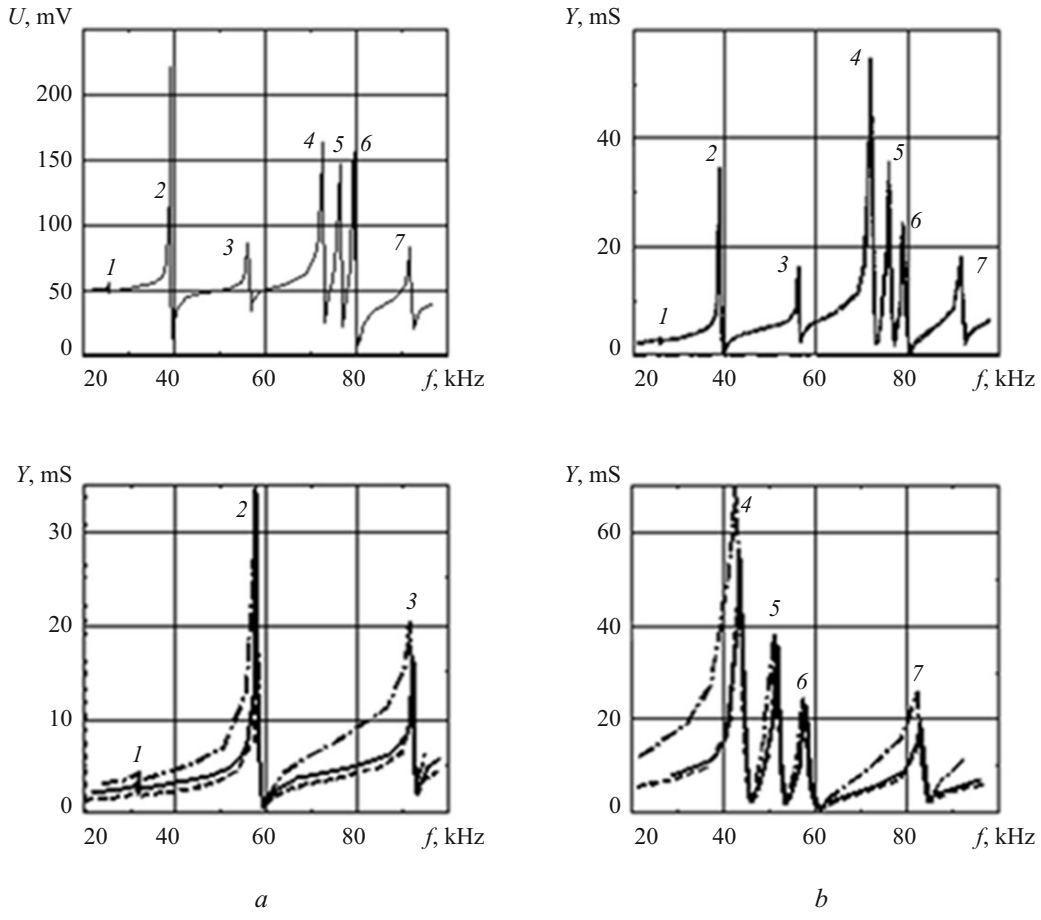

Fig. 3

a transfer element and the voltage drop across the piezoelectric element is measured, the admittance is calculated by the approximate formula

$$Y_{\text{pe}} = 2\pi f C(U_{R2} - U_{\text{pe}})/U_{\text{pe}}. \quad (6)$$

2. Admittance–Frequency Response of Piezoelectric Elements with Resistive and Capacitive Loads. When an electric current of ultrasonic frequency passes through a piezoelectric element and a series-connected resistor or capacitor, a phase shift occurs between current and voltage, affecting the results of measurements. The interaction of the capacitive and mechanical components of the voltage drop across elements of the measuring section of the advanced Mason circuit is well observed in multiresonance systems, such as a piezoceramic half-disk [21] where several electromechanical resonances of different intensity occur (Fig. 3) within a relatively narrow frequency range (20–100 kHz). Figure 3a shows the voltage drops across a pull-up resistor of 110 Ω (solid lines) or a fixed capacitor of 15,830 pF equal to the static self-capacitance of the semidisk (dashed lines). Figure 3b illustrates the admittance–frequency response of a half-disk with a resistor of 55 Ω or a capacitor of 15,830 pF [21]. A voltage of 100 mV was maintained at the input of the measuring circuit at all frequencies. Seven resonances of different intensity can be observed. The admittance peaks correspond to the peaks of the voltage drop. Increasing the capacitance of the load capacitor severalfold (to 105,840 pF) reduces the amplitude of the resonances, but does not change either the frequency response or the magnitude of the admittance. Moreover, the values of the admittance at different frequencies calculated with formulas (4) and (5) are practically equal (Fig. 3b).

Let us split the frequency range into two subranges: 20–60 kHz (Fig. 3c) and 60–100 kHz (Fig. 3d), and plot the admittance–frequency responses for three measuring circuits: (i) a pull-up resistor 110 Ω in the conventional Mason circuit (dash-and-dot line), (ii) a limiting resistor of 1000 Ω (dashed line), (iii) a pull-up resistor of 55 Ω (solid line) in the advanced Mason circuit. In case (i), the voltage drop across the piezoelectric element is determined approximately as the difference

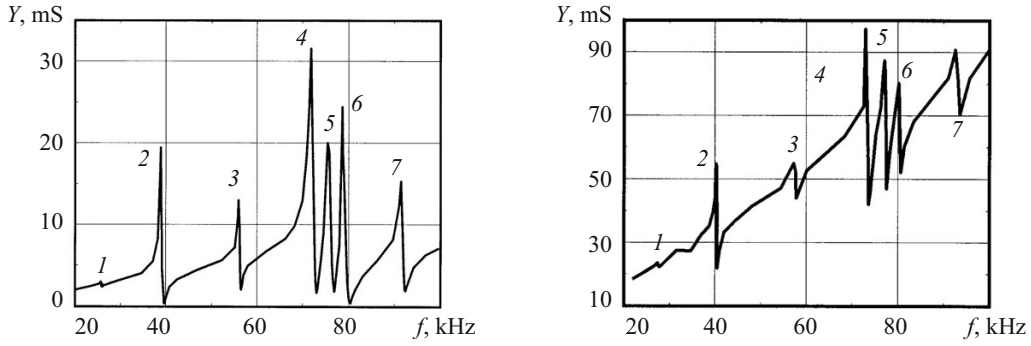

Fig. 4

between the input voltage and the voltage drop across the pull-up resistor. The admittance is calculated by the approximate formula (3). In case (ii), the voltage drop across the limiting resistor is determined approximately as the difference between the input voltage and the voltage drop across the piezoelectric element:

$$U_R = U_{R2} - U_{\text{pe}} \tag{7}$$

and the admittance is determined by the approximate formula

$$Y = \frac{U_{R2} - U_{\text{pe}}}{RU_{\text{pe}}}. \tag{8}$$

In case (iii), use is made of formula (4) because the voltage drop across the piezoelectric element and the pull-up resistor was measured in a circuit with a switch independently, sequentially, and with equal high accuracy.

Comparing Figs. 3c, d with Fig. 3b, it is easy to see that both the refined formula (4) and the approximate formulas (3) and (8) calculate the admittance of the piezoelectric element with satisfactory accuracy. The minimum admittances calculated with the different formulas are practically equal. The maximum difference produced by the formulas is between neighboring resonances. At many frequencies, formula (3) overestimates the admittance by almost 50%, whereas formula (8) underestimates the admittance at the same points by 10–15%. In frequency ranges near the resonances, except for the first, very weak one, formulas (4) and (8) yield very similar results.

Figure 4 shows the admittance–frequency response of a piezoceramic half-disk in two special cases of capacitive load: (i) a transfer capacitor of 600 pF (Fig. 4a) and (ii) a capacitor of 105,840 pF connected in parallel to the piezoelectric element with a pull-up resistor of 3 Ω (Fig. 4b). The approximate formulas (6) and (8) were used, respectively. Compared with other methods of excitation, a capacitor of low capacitance (much lower than the static self-capacitance) connected in series with the piezoelectric element reduced the amplitude of resonance by 30–50%, and the minima became shaper. Connecting a capacitor of high capacitance in parallel to the piezoelectric element increased the admittance of the resulting circuit severalfold, and the contribution of the capacitive component became predominant. The weak first resonance is detected poorly. The other resonances keep their positions and relative intensity. Thus, resonant phenomena in piezoceramics are determined by its electromechanical properties and it is difficult for external passive elements to affect them.

3. Phase Shifts between Voltage Components. As indicated above, introducing an additional switch to the Mason circuit allows measuring the voltage drop U_{pe} across the piezoelectric element Pe and the pull-up resistor R_{ld} or capacitor C_{ld} with equally high accuracy at any frequency f. The voltage drop $U_{\text{in}} = U_{R2}$ across the resistor $R2$ of the matching divider is supplied to the input of the measuring circuit. We have, thus, three voltage components: U_{in}, U_{pe}, and U_R or U_{c}. With three side lengths of a triangle known, we can use the cosine rule to calculate the vertex angles. For example, the angle opposite to the side U_{in} characterizes the phase shift between the voltage drop across the piezoelectric element and the voltage drop across the series-connected resistor or capacitor:

$$\cos\alpha = (U_{\text{pe}}^2 + U_R^2 - U_{\text{in}}^2) / (2U_{\text{pe}}U_R). \tag{9}$$

TABLE 1

Frequency	35.967	37.933	38.479	38.742	38.846	39.027	39.188	39.686
U_{pe}, mV	94	86	73	42	34	64	84	98
U_R, mV	25	36	50	65	64	45	26	3
U_{in}, mV	100	100	100	100	100	100	100	100
Y, mS	4.83	7.61	12.45	28.14	34.22	12.78	5.63	0.487
$\cos\alpha$	–0.1147	–0.2112	–0.2974	–0.7346	–1.0910	–0.6711	–0.5192	–0.6633
α	–83°20′	–77°50′	–72°40′	–42°40′	—	–47°50′	–58°30′	–48°50′
α^*	–78°	–77°	–73°	–40°	—	–44°	–54°	–55°
$\cos\beta$	0.3578	0.5417	0.7171	0.9585	—	0.8811	0.6962	0.68
β	69°	57°10′	44°10′	16°40′	—	28°10′	45°50′	47°30′
β^*	62°	58°	44°	18°	—	26°	45°	—
$\cos\gamma$	0.9687	0.9360	0.8787	0.8975	—	0.8430	0.975	0.9996
γ	14°10′	20°30′	28°30′	26°10′	—	19°20′	13°	1°40′
γ^*	16°	21°	29°	25°	—	18°	13°	—
$\alpha+\beta+\gamma$	179°50′	179°50′	180°	180°10′	—	179°20′	180°10′	180°40′
$\alpha^*+\beta^*+\gamma^*$	180°	182°	180°	183°	—	180°	184°	—

Table 1 summarizes the results of measurement and calculation for the piezoceramic half-disk at eight arbitrarily chosen frequencies (in kHz) near its first strong resonance. The calculated angles are negative at all frequencies, which means that they are measured from 180°, i.e., are obtuse. The angle α is formed by the sides U_{pe} and U_R of the triangle. It is opposite to the side U_{in} and characterizes the phase shift between the voltage drop across the piezoelectric element and the electric current through it. The current through and the voltage drop across a resistor are known to be in phase. The angle β is formed by the sides U_{in} and U_R of the triangle. It is opposite to the side Upe and characterizes the phase shift between the input voltage and the current through the piezoelectric element. The angle γ is formed by the sides U_{in} and U_{pe} of the triangle. It is opposite to the side U_R and characterizes the phase shift between the input voltage and the voltage drop across the piezoelectric element.

The asterisk indicates the angles measured with a protractor after geometrical construction. The difference between the results obtained by graphical measurement and calculation does not exceed 10%. The calculated value of $\cos\alpha$ at one point appears greater than unity, which is meaningless and due to the errors of measurement of voltage drops. It is the frequency of the maximum admittance at which there are no phase shifts. The admittance was calculated by formula (4). The two bottom rows of Table 1 give the sums of calculated and measured angles which are equal or close to 180°.

It can be seen from Table 1 that as the frequency tends to the resonance at 38,846 kHz, the phase angle between the voltage drops U_{pe} and U_R increases and tends to 180° rather than to zero suggested by physical reasoning. The reason is that changing the switch in the advanced circuit from the first position to the second one reverses the direction of the current through

TABLE 2

Frequency	38.551	38.749	39.035	39.112	39.270	39.377	39.450	39.698
U_{pe}, mV	20	12	44	105	200	170	140	96
U_c, mV	79	90	132	175	210	100	60	12
U_{in}, mV	100	100	100	100	100	100	100	100
Y, mS	15.14	28.89	11.6	6.493	4.094	2.302	1.678	0.493
$\cos\alpha$	–1.0629	–0.8129	0.8492	0.8612	0.8821	0.85	0.7857	–0.2783
α	—	–35°40′	31°40′	30°30′	28°	31°50′	38°20′	–79°40′
α^*	—	–27°	38°	30°	27°	32°	42°	–75°
$\cos\beta$	1.0026	0.9976	0.9655	0.8457	0.3357	–0.4451	–0.5	0.387
β	—	4°	15°10′	32°30′	70°20′	–65°30′	–60°	67°10′
β^*	—	4°	18°	33°	68°	116°	118°	69°
$\cos\gamma$	1.0397	0.8517	–0.6236	–0.4671	0.1405	0.850	0.9286	0.9933
γ	—	31°40′	–51°25′	–62°50′	81°50′	31°50′	21°50′	6°40′
γ^*	—	25°	127°	117°	82°	35°	25°	9°
$\alpha+\beta+\gamma$	—	180°	177°	180°	180°	180°	180°	—
$\alpha^*+\beta^*+\gamma^*$	—	186°	183°	183°	177°	183°	186°	—

the piezoelectric element and the resistor. This fact by no means affects the electromechanical processes in the piezoelectric element, but it should be taken into account when interpreting the results.

Table 2 summarizes the results of measurement and calculation for the same half-disk in the same frequency range after replacement of the pull-up resistor of 55 Ω by a capacitor of 15,830 pF. The admittance was calculated by formula (5). Dashes in some table cells represent cases where the sum of two side lengths of the triangle is less than the length of the third side or one of the sides is much shorter than the other two. Eight frequencies were selected arbitrarily near the maximum and minimum admittances. After the replacement of the resistive load by the capacitive load, additional phase shifts occur between the voltage drops across the piezoelectric element (U_{pe}), capacitor (U_c), and the output resistor of the matching divider (U_{in}).

In both tables, the calculated and measured values are very similar, though both calculations and geometrical constructions are approximate procedures. The main source of errors is the voltmeter that measures the voltage drop. We used a V3-38 millivoltmeter of precision class 4. This means that if its full scale is, for example, 100 mV, then the error is ±4 mV. If the voltage measured on this scale is 30 mV, then the relative error (±4 mV/30 mV) 100% = 13.3%. The accuracy of measurement can be enhanced by either timely switching between voltmeter scales or measuring such levels of voltage at which the pointer of the device is near the scale edge.

The tables are supported by the phase–frequency responses of the piezoceramic self-disk (Fig. 5) obtained by geometrical construction. Curves *a*, *b*, and *g* correspond to angles α, β, and γ, respectively.

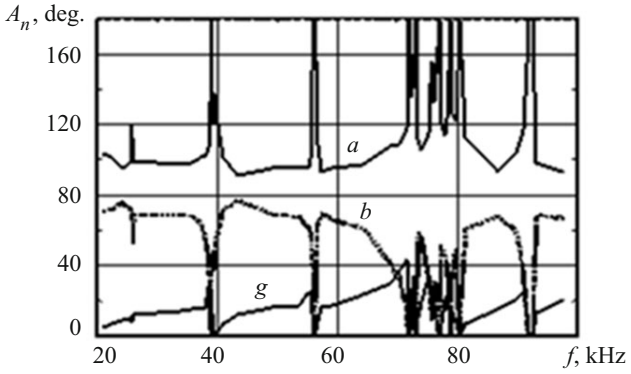

Fig. 5

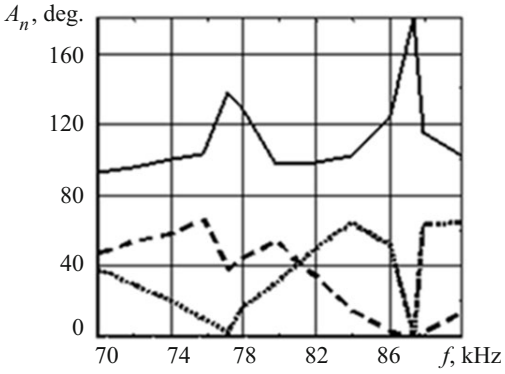

Fig. 6

The curves demonstrate that the phase shift between the voltage drop across the piezoelectric element and the electric current through it (curve *a*) between neighboring resonances tends to 100°. Between a resonance and the corresponding antiresonance, the phase shifts sharply change from 180 to 120° and again to 180°. The angles β and γ pass through nearly zero minima between resonances and respective antiresonances. Between neighboring resonances, these angles tend to 65–70° and 10–15°, respectively.

The measured voltages U_{in}, U_{pe}, U_R and the respective frequencies were entered into the computer to then display the admittance components, cosines of phase angles, angles themselves, and components of active, reactive, and instantaneous power. It appeared that the presence or absence of nonlinearity mentioned in [27–29] is due to an increase or a decrease in instantaneous power as a resonance is approached. However, this is beyond the scope of the present paper and should be studied separately.

4. Sequential Measurement of Amplitudes and Phases of Voltage. The cosine rule and formula (9) can also be used in sequential measurement of the voltage drops across the piezoelectric element and the pull-up resistor. The series-connected piezoelectric element and resistor were connected to the output resistor of the matching divider in the conventional Mason circuit so that either the resistor or the piezoelectric element was grounded. The voltage–frequency response was first recorded on one of them and then on the other.

These curves were then plotted on the same frequency axis. The figure was printed out, and the ordinates U_{pe} and U_R were measured at specially chosen frequencies. The third side U_{in} of the triangle was kept at constant amplitude during the measurements. The experimental data were treated in the same way as for the advanced Mason circuit. Table 3 and Fig. 6 illustrate the above-said for the piezoelectrically strong third resonance of a 22.2×18.2×15.8 mm thin-walled cylindrical shell made of TsTBS-3 piezoceramics.

Here, as in the piezoceramic half-disk, the phase shifts change most sharply at resonant and antiresonant frequencies. Between these points, the phase shift between the voltage drop across the piezoelectric element and the current through it is the same as between neighboring resonances. This phase shift is caused by the self-capacitance and is close to 90°.

The amplitudes of the admittance of piezoelectric elements at resonant frequencies can also be determined using the shunting effect [20]: the input impedance of the piezoelectric element somewhat shunts the output resistor $R2$ of the divider when they are connected in parallel. The shunting effect of the piezoelectric element is the most noticeable at the resonant frequencies, and the voltage drop across it decreases by a factor of K compared with low frequencies at which the shunting effect is very weak. The resonant admittance Y_{r} can be determined by the approximate formula

$$Y_{\text{r}}[\text{mS}] = 10^3 (K-1)/R2[\Omega],$$

which is derived from Ohm's law.

Neither the shunting method nor the piezotransformer transducer method [13, 14] can be used to determine the admittance of the piezoelectric element at an antiresonance.

Conclusions. Studying the forced electromechanical vibrations of a thin piezoceramic half-disk in some frequency range using several circuits for electric excitation of vibrations, we have drawn the following conclusions.

TABLE 3

f, kHz	70	74	75.74	77.13	78	80.98	83.94	86	8l.91	90
Y, mS	11.81	21.6	40.7	145	68.9	9.09	2.67	0.66	0.47	1.34
α	91°30′	98°	100°30′	130°30′	136°10′	96°30′	99°20′	113°30′	125°40′	107°
β	36°10′	20°30′	13°30′	2°40′	4°40′	41°40′	65°10′	62°50′	52°	65°20′
γ	48°20′	60°40′	67°20′	46°10′	39°10′	41°40′	15°20′	3°40′	2°20′	8°
α^*	93°	101°	103°	138°	128°	97°	102°	125°	115°	102°
β^*	38°	20°	10°	2°	7°	41°	64°	52°	63°	64°
γ^*	47°	58°	66°	38°	45°	41°	14°	3°	2°	14°

1. The sequential measurement of the voltage drops across the piezoelectric element and the pull-up resistor or the capacitor in the advanced Mason circuit with a switch allows determining the admittance components and phase shifts at any frequency with accuracy sufficient for engineering purposes.

2. The circuit with a limiting resistor quite accurately measures the admittance components in the frequency range between a resonance and the respective antiresonance and near a resonance.

3. Using a capacitor of low capacitance as a transfer element improves the accuracy of measuring antiresonant frequencies.

4. The resonant properties of piezoceramics are determined by the internal electromechanical processes and are independent of the effect of external passive elements.

REFERENCES

1. V. A. Akopyan, A. N. Solov'ev, and S. N. Shevtsov, *Methods and an Algorithm for Determining the Full Set of Compatible Material Constants of Piezoceramic Materials* [in Russian], Izd. YuFU, Rostov-on-Don (2008).
2. O. Bezverkhii, L. Zinchuk, and V. Karlash, „Effect of the mode of electric loading and direct current or voltage on the vibrations of piezoelectric vibrators," *Fiz.-Mekh. Model. Inform. Tekhnol.*, **18**, 9–20 (2013).
3. I. A. Glozman, *Piezoceramics* [in Russian], Energiya, Moscow (1972).
4. GOST 12370-72. *Piezoceramic Materials*, *Testing Methods* [in Russian], Izd. Standartov, Moscow (1973).
5. V. L. Zemlyakov and S. N. Klyuchnikov, "Determination of the parameters of piezoceramic elements from amplitude measurements," *Measur. Techn.*, **53**, No. 3, 301–304 (2010).
6. A. M. Kalashnikov and Ya. V. Stepuk, *Basics of Radio Engineering and Radar Ranging* [in Russian], Voenizdat, Moscow (1962).
7. V. L. Karlash, "Electromechanical vibrations of a piezoceramic hollow spheroid with a polar notch," *Int. Appl. Mech.*, **46**, No. 5, 540–545 (2010).
8. V. L. Karlash, "Methods for determining the coupling coefficients for and energy loss in piezoceramic vibrators," *Akust. Visn.*, **15**, No. 4, 24–38 (2012).
9. H. W. Katz (ed.), *Solid State Magnetic and Dielectric Devices*, Wiley, New York (1959).
10. I. E. Tamm, *Fundamentals of the Theory of Electricity*, Mir, Moscow (1966).

11. V. M. Sharapov (ed.), I. G. Minaev, Yu. Yu. Bondarenko, T. Yu. Kisil', M. P. Musienko, S. V. Rotte, I. B. Chudaeva, et al., *Piezoelectric Transducers* [in Russian], ChGTU, Cherkassy (2004).
12. N. A. Shul'ga and A. M. Bolkisev, *Vibrations of Piezoelectric Bodies* [in Russian], Naukova Dumka, Kyiv (1990).
13. M. O. Shul'ga and V. L. Karlash, *Resonant Electromechanical Vibrations of Piezoelectric Plates* [in Ukrainian], Naukova Dumka, Kyiv (2008).
14. M. O. Shulga and V. L. Karlash, "Measuring the admittance of piezoceramic elements in Mason's quadripole circuit and its modifications," in: *Abstracts 4th Int. Sci.-Tech. Conf. on Sensors*, *Devices*, *and Systems*, Cherkasy–Gurzuf (2008), pp. 54–56.
15. M. O. Shul'ga and V. L. Karlash, "Amplitude–phase characteristics of radial vibrations of a thin piezoceramic disk at resonances," *Dop. NAN Ukrainy*, No. 9, 80–86 (2013).
16. R. Holland and E. P. Eer Nisse, *Design of Resonant Piezoelectric Devices*, M.I.T.Press, Cambridge (1969).
17. "IRE Standards on piezoelectric crystals: Measurements of piezoelectric ceramics. 1961," *Proc. IRE*, **49**, 1161–1169 (1961).
18. V. Karlash, "Longitudinal and lateral vibrations of a planar piezoceramic transformer," *Jpn. J. Appl. Phys.*, **44**, No. 4A, 1852–1856 (2005).
19. V. L. Karlash, "Resonant electromechanical vibrations of piezoelectric plates," *Int. Appl. Mech.*, **41**, No. 7, 709–747 (2005).
20. V. L. Karlash, "Planar electroelastic vibrations of piezoceramic rectangular plate and half-disk," *Int. Appl. Mech.*, **43**, No. 5, 547–553 (2007).
21. V. L. Karlash, "Admittance–frequency response of a thin piezoceramic half-disk," *Int. Appl. Mech.*, **45**, No. 10, 1120–1126 (2009).
22. V. L. Karlash, "Energy losses in piezoceramic resonators and its influence on vibration's characteristics," *Electronics and Communication*, **19**, No. 2 (79), 82–94 (2013).
23. V. L. Karlash, "Forced electromechanical vibrations of rectangular piezoceramic bars with sectionalized electrodes," *Int. Appl. Mech.*, **49**, No. 3, 360–368 (2013).
24. I. F. Kirichok, "Resonant vibrations and self-heating of a clamped flexible thermoviscoelastic beam with piezoactuators," *Int. Appl. Mech.*, **50**, No. 4, 421–429 (2014).
25. A. V. Mezheritsky, "Quality factor of piezoceramics," *Ferroelectrics*, **266**, 277–304 (2002).
26. A. V. Mezheritsky, "Elastic, dielectric and piezoelectric losses in piezoceramics; how it works all together," *IEEE Trans. Ultrason.*, *Ferroelect.*, *Frec. Contr.*, **51**, No. 6, 695–797 (2004).
27. N. A. Shul'ga, L. O. Grigor'eva, and N. O. Babkova, "Electrically excited nonstationary vibrations of thin circular piezoelectric plates," *Int. Appl. Mech.*, **50**, No. 4, 406–411 (2014).
28. K. Uchino, J. H. Zheng, Y. H. Chen, et al., "Loss mechanisms and high power piezoelectrics," *J. Mat. Sci.*, **41**, 217–228 (2006).
29. K. Uchino, Yu. Zhuang, and S. O. Ural, "Loss detertmination methodology for a piezoelectric ceramic: new phenomenological theory and experimental proposals," *J. Adv. Dielectr.*, **1**, No. 1, 17–31 (2011).
30. S. O. Ural, S. Tunodemir, Yu. Zhuang, and K. Uchino, "Development of a high power piezoelectric characterization system and its application for resonance/antiresonance mode characterization," *Jpn. J. Appl. Phys.*, **48**, 506–509 (2009).